DOI: 10.1021/ma1003198

Macromolecules
ARTICLE

Preparation of Polymeric SWNT−Liquid Crystal Composites Using a Polymerizable Surfactant

Yoon Sung Kwon, Byung Mun Jung, Hyunpyo Lee, and Ji Young Chang*

Department of Materials Science and Engineering, College of Engineering, Seoul National University, Seoul 151-744, Korea

Received February 8, 2010; Revised Manuscript Received May 19, 2010

ABSTRACT: Polymeric carbon nanotube (CNT)−liquid crystal composites were prepared using single-walled CNTs (SWNTs) and a polymerizable surfactant (dodecyldimethylammonium ethyl methacrylate, DDAM). The pristine SWNTs were dispersed in a lyotropic liquid crystal (LC) of DDAM (70 wt % in water). The bare lyotropic LC of DDAM and the dispersions showed columnar hexagonal phases. In X-ray diffraction analysis, the *d*-spacings were increased as the pristine SWNT concentration was increased up to 0.15 wt %, indicating that the pristine nanotubes were well incorporated in the hexagonal LC phase where they induced a swelling of the structure. The dispersions were photopolymerized to give polymeric composites. With increasing pristine SWNT concentration, the electrical resistivities of the composites continuously decreased, while their dielectric constants increased. The method reported herein provides a facile way to prepare a polymeric CNT−LC composite that combines the properties of both LCs and SWNTs.

Introduction

Carbon nanotubes (CNTs) have great potential applications in many fields of nanotechnology due to their unique mechanical, thermal, and electrical properties.[1−6] Nanocomposites from CNTs with polymers and other organic materials have been reported showing improved properties.[7−10] However, the effects of CNTs are often restricted because of their strong aggregations. The very strong van der Waals force between the nanotube walls tightly binds them into nanotube bundles, which are in turn aggregated into large particles.[11] They have very poor solubility in most solvents and matrix materials.

Various techniques have been exploited to achieve homogeneous dispersion of CNTs in nanocomposites. Mechanical mixing by twin-screw extruder[12] and ball milling[13] are used to break large aggregates into small bundles, but they struggle to break them into single nanotubes, especially for single-walled CNTs (SWNTs). The widely applied method using a surfactant is normally effective when CNTs are dispersed in hydrophilic solvents or polymers.[14,15] This process is conducted by physical adsorption of surfactant molecules onto the surface of CNTs. The large nanotube bundles are debundled while surfactants are wrapping the single nanotubes or thin bundles. The molecules having a pyrene unit are also used as dispersant,[16] and biomolecules such as DNA[17] and polysaccharide[18] are also known to disperse CNTs by extending their long chains around the surface. Since these methods do not induce defects or changes to the chemical structures of the nanotube surfaces, the physical properties of CNTs are not damaged. Chemical modification is another dispersing method.[19−22] In this method, solvents or matrix soluble compounds having reaction sites are grafted onto the surface of CNTs through a covalent bond. Dispersing moieties are thus stably attached to the surface of nanotubes so that they can form a stable dispersion. However, the chemical structures are partly degraded due to the chemical reactions, thereby damaging the physical and chemical properties of nanotubes.

CNTs have large aspect ratios and exhibit their remarkable properties along the tube axis. Therefore, the realization of uniform alignment of nanotubes is crucial for them to manifest their unique features in nanocomposites. Several methods have been developed for aligning dispersed nanotubes. Electric or magnetic field-induced alignment was reported as an effective method.[23] Electrospinning can be used to obtain aligned nanotube-embedded nanofibers.[24,25] Applying shear force to the composite film is another simple method to achieve an anisotropic film.[26] While these techniques utilize external force, some methods induce spontaneous alignment using an inherent anisotropic structure of a matrix material. For example, studies have reported using LCs as self-organizing nanotemplates for CNT alignment.[27−37] Most CNT− LC composites, however, suffer limitations in actual applications due to their thermal and mechanical instability and the ease with which they are deformed by external force.

In this work, we prepared physically stable, polymeric CNT−LC composites using a polymerizable LC surfactant, dodecyldimethylammonium ethyl methacrylate (DDAM). DDAM presents in various morphologies such as micellar, columnar hexagonal, bicontinuous, and lamellar phase, depending on the concentration in water.[38,39] Our approach to the preparation of a polymeric CNT−LC composite is schematically shown in Figure 1. SWNTs are first dispersed in a lyotropic LC of DDAM. Subsequent polymerization of the surfactant molecules adsorbed onto the surface of CNT in the LC state produces the composite. This approach constitutes a valuable route for the synthesis of polymeric composite materials containing well-dispersed and aligned CNTs.

Experimental Section

Materials and Instrumentation. Pristine single-walled carbon nanotubes (SWNTs) were purchased from Hanhwa Nanotech (ASP-100T, synthesized by arc-discharge method).

*Corresponding author: Tel +82-2-880-7190, Fax +82-2-885-1748, e-mail jichang@snu.ac.kr.

 Published on Web 05/26/2010

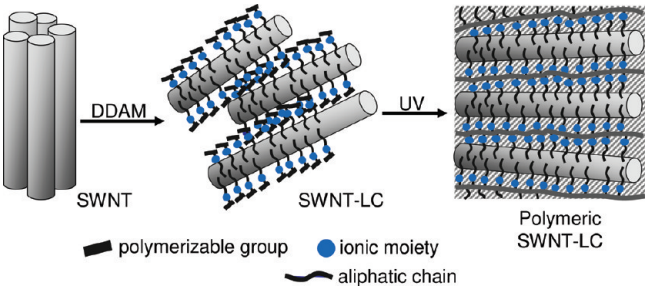

Figure 1. Schematic representation of photopolymerization of a CNT−lyotropic LC composite.

12-Bromododecane and 2-(dimethylamino)ethyl methacrylate (98%) were purchased from Aldrich. 2,2-Dimethoxy-2-phenylacetophenone (DMPA) was purchased from TCI. Ultrapure water (18.3 MΩ·cm) was obtained from a water purification system (Human Power I+, Human Corp.).

Raman spectroscopy analysis was conducted by Raman spectrometer T64000 (Horiaba Jobin Yvon). Zeta-potential was measured by dynamic laser light scattering (DLS, ELS-Z, Otsuka Electronics Co., Ltd.). The samples were prepared by dispersing carbon nanotubes in ultrapure water. The ^{1}H NMR spectrum was recorded on a Bruker Avance DPX-300. Polarized optical microscopy (POM) was performed by a Leica DMLP equipped with a Mettler Toledo FP82HT heating stage and a Mettler Toledo FP90 central process controller. X-ray diffractograms were obtained with the use of a Bruker Nanostar small-angle X-ray scattering (SAXS) system (Cu Kα radiation, λ = 1.54 Å). The samples were prepared by filling the thin glass capillaries (1.0 mm diameter) with compounds. Differential scanning calorimetry (DSC) was performed on a differential scanning calorimeter (Q10, TA Instruments) at the scanning rate of 10 °C/min with nitrogen gas purging. The electrical resistivity was measured by a four-point probe technique (FPP-5000, Chang Min Tech., Co.). The obtained raw data were sheet resistance and converted to resistivity by multiplying the thickness of the sample. The dielectric constants were measured by a precision impedance analyzer (4294A equipped with 16451B, 16089E, N6314A, and N6315A, Agilent Technologies). The data were recorded at 10 MHz.

Synthesis of Dodecyldimethylammonium Ethyl Methacrylate (DDAM). DDAM was prepared by reacting (dimethylamino)-ethyl methacrylate with 12-bromododecane according to the method previously reported.[38] (Dimethylamino)ethyl methacrylate (7.87 g, 50.0 mmol) and 12-bromododecane (10.4 g, 41.7 mmol) were dissolved in acetone (200 mL). A little amount of 4-methoxyphenol was added to the solution as a polymerization inhibitor. The mixture was stirred at 50 °C for 4 days. After acetone was evaporated, the product was isolated by precipitation in diethyl ether and further purified by recrystallization from ethyl acetate to give white solids: yield 12.2 g (72%). ^{1}H NMR (300 MHz, DMSO-d_6): δ 6.08 (s, 1H, CH=C), 5.76 (s, 1H, CH=C), 4.52 (t, 2H, COO−CH_2−), 3.73 (t, 2H, −CH_2−N), 3.11 (s, 6H, N−$(CH_3)_2$), 1.91 (s, 3H, C−CH_3), 1.68 (m, 2H, −CH_2−CH_2N), 1.25 (br, 18H, CH_3−$(CH_2)_9$−), 0.86 (s, 3H, −CH_3).

Oxidation of Pristine SWNTs. Pristine SWNTs (100 mg) were added to a mixture of nitric acid (70%) and sulfuric acid (98%) (100 mL, 1:3 v/v). The mixture was sonicated using a bath sonicator (37 kHz) at 40 °C for 4 h. After cooling the mixture to room temperature, deionized water (200 mL) was added, and the mixture was filtered through a 20 nm pore alumina filter membrane. The residue was washed several times by distilled water until the filtrate became neutral. The collected oxidized SWNTs were dried in vacuo; yield: 40 mg (40%).

Dispersion of SWNTs in Lyotropic Liquid Crystals. A calculated amount of DDAM was added to a dispersion of SWNTs (0−0.2 wt %) in distilled water and then sonicated for 4 h.

Scheme 1. Synthesis of DDAM

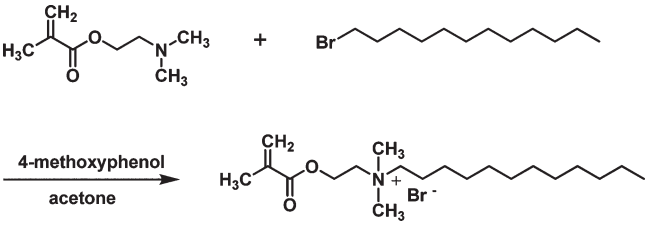

Scheme 2. Schematic Representation of the Dispersion Process of the SWNTs Following DDAM Addition in Water

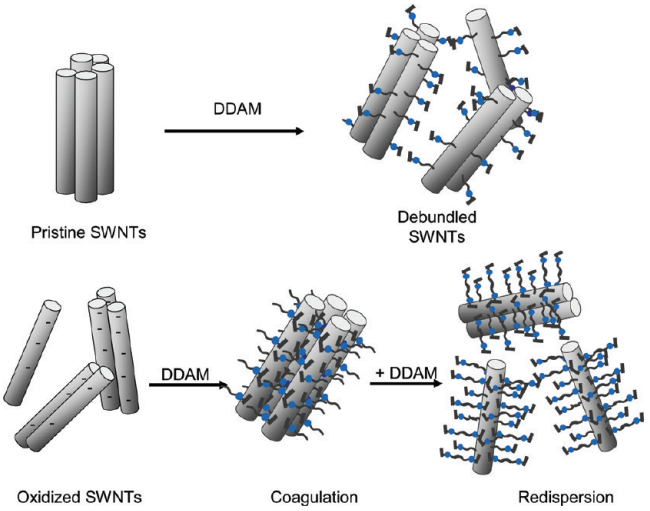

Photopolymerization. For the POM study, a mixture of an aqueous dispersion of SWNTs, DDAM (70 wt %), and a photoinitiator (DMPA, 0.5 wt %) was placed between a glass slide and a coverslip and polymerized by photoirradiation with a high-pressure UV lamp (mercury arc lamp, 3 mW/cm^2) at room temperature for 10 min. For resistivity and dielectric constant measurements, pellet-type samples were prepared by photopolymerizing the mixture at room temperature for 5 h in a cylinder-shaped Teflon mold (2 cm diameter).

Results and Discussion

Dispersion of Pristine SWNTs and Oxidized SWNTs in Water with DDAM. DDAM was synthesized according to Scheme 1 as previously reported.[38] Pristine SWNTs were oxidized in nitric and sulfuric acids under sonication to obtain hydrophilic surfaces. In the Raman spectrum, pristine SWNTs showed strong G-band peak at 1600 cm^{-1}, indicating that they had a graphene structure with few defects, while oxidized SWNTs showed largely increased intensity of D-band (~1300 cm^{-1}). After oxidation, the zeta-potential value was shifted from −22.91 mV (pristine SWNTs) to −45.44 mV (oxidized SWNTs), suggesting the formation of carboxylic groups.

The dispersibility of pristine and oxidized SWNTs was tested by dispersing 1 mg of SWNTs in 2 mL of water. After adding SWNTs to water, the mixture was sonicated for 1 h. The pristine SWNTs showed very poor dispersibility in water. After addition of DDAM (50 mg) to the pristine SWNT dispersion, the large nanotube agglomerates were shrunken and the dispersion property was improved. Subsequent sonication produced a stable black dispersion. The oxidized SWNTs formed a homogeneous dispersion in water. Interestingly, however, the coagulation occurred instantly when 5 mg of DDAM was added. This result was

attributed to the interaction of the cationic parts of the surfactants with the negatively charged surface of the oxidized SWNTs, which exposed the hydrophobic alkyl chains to water. The coagulated dispersion was sonicated for 1 h, but the large agglomerates were not redispersed. A stable colloidal dispersion was obtained by addition of more of DDAM (50 mg) and further sonication. This result suggested that alkyl chains of the surfactants interacted with the initially formed hydrophobic surface of the oxidized SWNT such that their cationic parts became exposed to water. The dispersion process of the SWNTs following DDAM addition is schematically shown in Scheme 2.

The surface property changes of pristine SWNTs and oxidized SWNTs in the addition process of DDAM were investigated by zeta-potential measurement. The samples were prepared by adding 2 mg of DDAM to a dispersion of pristine SWNTs or oxidized SWNTs (1 mg) in water (3 mL). The zeta-potentials of pristine SWNTs and oxidized SWNTs were −22.91 and −45.44 mV, respectively. The negative zeta-potential of the pristine SWNTs was mainly attributed to the defect sites. When DDAM was added, the negative value was converted to a positive value (+13.83 mV), suggesting that the cationic charges of the surfactants were exposed to water. The oxidized SWNT−DDAM mixture also showed a positive value (+6.75 mV) but smaller than that of the pristine SWNT−DDAM mixture. This result was attributed to the effect of the Coulombic force in causing most of the surfactants to be adsorbed in the nanotube surface with cationic parts inside and alkyl chains outside. These surfactants where then surrounded by surplus surfactants that formed a second layer with cationic parts outside.

Polarized Optical Microscopy (POM) Study. The liquid crystalline phase and the dispersion state of SWNTs were investigated by POM. As reported in the literature,[40] the bare lyotropic LC (70 wt % of DDAM) showed a conical texture which was typical for a columnar hexagonal phase. Figure 2 shows the POM images of the pristine SWNT−lyotropic LC composites with nanotube concentrations ranging from 0.05 to 0.20 wt %. With increasing nanotube concentration, the nanotube bundles became visible. Figure 3 shows the POM images of the oxidized SWNT−lyotropic LC composites.

Polymerization of the SWNT−lyotropic LC composites was carried out by photoirradiation with a high-pressure UV lamp. For the POM study, a composite containing 0.5 wt % of SWNT and 70 wt % of DDAM was placed between a slide glass and a coverslip and polymerized by photoirradiation with a high-pressure UV lamp. Figure 4 shows the POM images of the polymerized samples. The polymeric composite showed a similar texture to that of the polymerized bare LC (70 wt % of DDAM) (Figure 4a), suggesting the

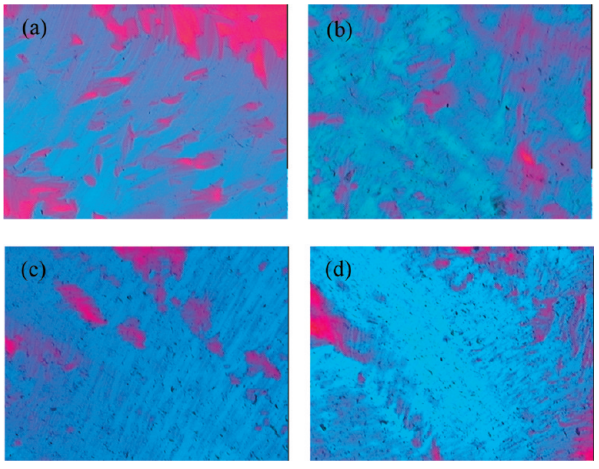

Figure 2. POM images of the pristine SWNT−lyotropic LC composites with a nanotube concentration of (a) 0.05, (b) 0.10, (c) 0.15, and (d) 0.20 wt %.

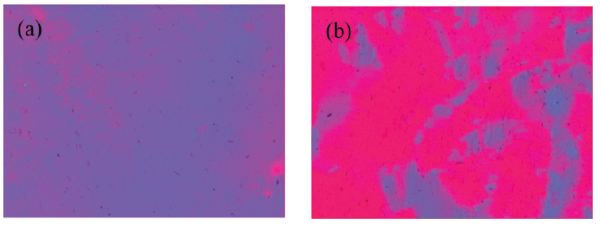

Figure 3. POM images of the oxidized SWNT−lyotropic LC composites with a nanotube concentration of (a) 0.05 and (b) 0.10 wt %.

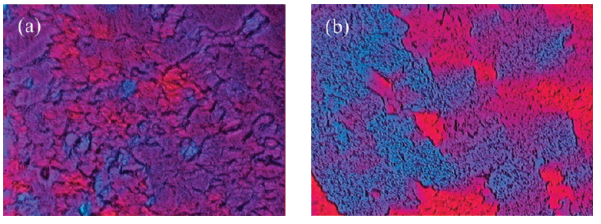

Figure 4. POM images of (a) the polymerized bare lyotropic LC (70 wt % of DDAM) and (b) the polymeric composite with 0.05 wt % of pristine SWNTs.

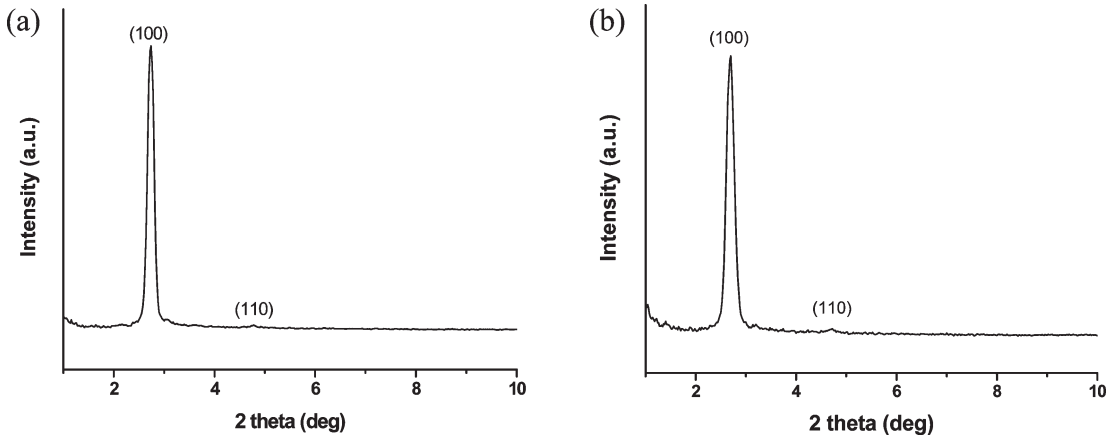

Figure 5. X-ray diffractograms of (a) the bare lyotropic LC (70 wt % of DDAM) and (b) the 0.05 wt % pristine SWNT−lyotropic LC composite.

absence of any significant phase separation during the polymerization.

X-ray Diffraction Study. The diffractogram of the bare LC (70 wt % of DDAM) showed two peaks with *d*-spacings of 32.21 and 18.46 Å. These reflections were indexed as (100) and (110) reflections of a columnar hexagonal lattice (Figure 5a).[40] In the diffractogram of the 0.05 wt % pristine SWNT composite, two peaks were also observed at *d*-spacings of 32.68 and 18.70 Å, corresponding to (100) and (110) reflections, respectively (Figure 5b). The d_{100}-spacing of the composite was 0.47 Å larger than that of the bare LC, indicating that the LC structure was swollen due to the incorporation of the nanotubes into the columnar hexagonal structures. The measurements were performed as the pristine SWNT concentration was increased from 0.05 to 0.2 wt %. The d_{100}-spacing increased steadily from 32.21 Å for the bare LC to 33.43 Å at 0.15 wt % concentration (Figure 6), but then decreased to 32.93 Å at 0.2 wt %. The increased *d*-spacing up to 0.15 wt % indicated that the pristine nanotubes were well incorporated in the hexagonal LC phase where they induced a swelling of the structure. At a higher concentration, however, the nanotubes probably aggregated, which reduced the concentration of the nanotubes incorporated within the LC structure.

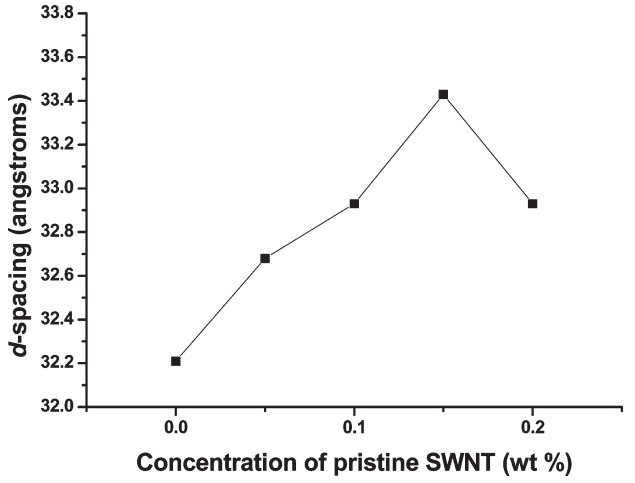

Figure 6. *d*-spacing of (100) reflection vs pristine SWNT concentration in the composite.

Polymerization changed the LC structure of DDAM from a columnar hexagonal to a lamellar structure as previously reported.[40] After polymerization, the X-ray diffractogram showed two peaks corresponding to (100) and (200) reflections with *d*-spacings of 34.20 and 17.24 Å, respectively (Figure 7a). The composite with 0.05 wt % of pristine SWNTs also showed the same structural change. The d_{100}- and d_{200}-spacings of the polymeric composite were 34.74 and 17.72 Å, respectively (Figure 7b).

Thermal Properties of Polymeric Composites. The thermal properties of the polymeric composites were studied by DSC. Figure 8 shows the differential scanning calorimetry (DSC) thermograms of DDAM and a polymeric composite with pristine SWNTs. Pure DDAM exhibited several transition peaks upon heating and cooling, including the melting transition

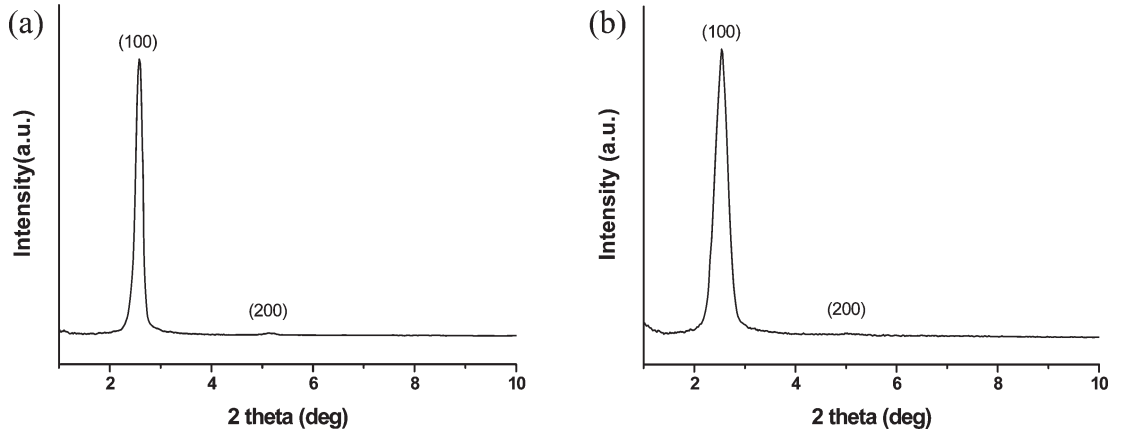

Figure 7. X-ray diffractograms of (a) the polymerized bare lyotropic LC (70 wt % of DDAM) and (b) the polymeric 0.05 wt % pristine SWNT−lyotropic LC composite.

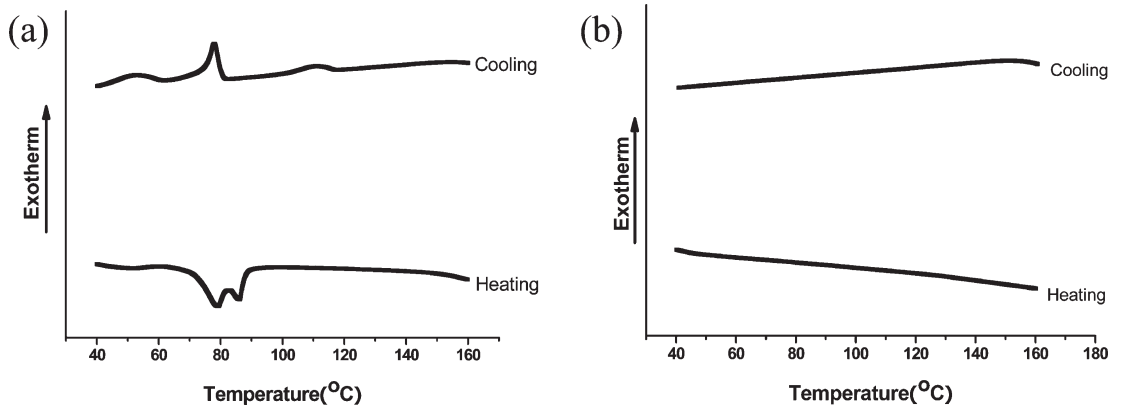

Figure 8. DSC thermograms of (a) DDAM and (b) the polymeric composite containing 0.10 wt % of pristine SWNT.

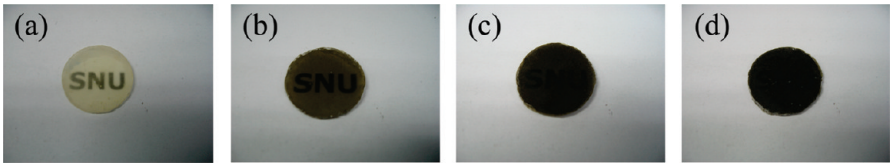

Figure 9. Pellet-type polymeric composites containing (a) 0.0, (b) 0.025, (c) 0.05, and (d) 0.10 wt % of pristine SWNT.

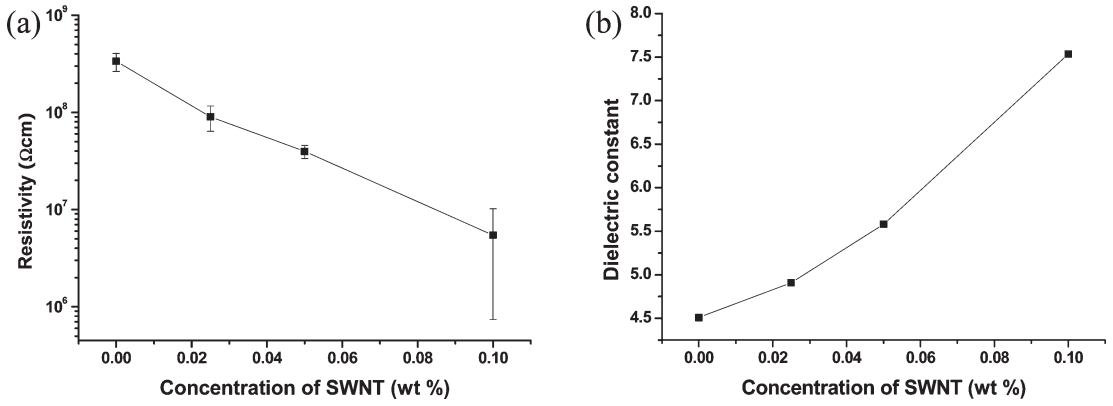

Figure 10. (a) Electrical resistivity vs pristine SWNT concentration. (b) Dielectric constant vs pristine SWNT concentration.

at 88 °C. The polymeric composite with 0.10 wt % of pristine SWNTs showed no transition peaks up to 170 °C, indicating that all the DDAM molecules had participated in the polymerization.

Electrical Properties. For resistivity and dielectric constant measurements, pellet-type samples were prepared by photopolymerizing the LC−SWNT composites at room temperature for 5 h in a cylinder-shaped Teflon mold (2 cm diameter). Figure 9 shows photographs of the polymeric composites with various concentrations (0.0, 0.025, 0.05, and 0.10 wt %). The electrical resistivity of the composites continuously decreased with increasing pristine SWNT concentration from 3.4×10^8 Ω·cm for the bare sample to 5.5×10^6 Ω·cm for the pristine SWNT composite at 0.1 wt % (Figure 10a). Although the resistivity was decreased 60-fold times by the addition of 0.1 wt % of pristine SWNTs, the value remained sufficiently high for the composition to be considered an insulator. This was attributed to a concentration that was insufficient for percolation of CNTs in the matrix and/or to the more semiconducting, rather than metallic, character of the CNTs.

The pristine nanotubes have abundant π-electrons that tend to be localized in a certain direction under an electric field. Therefore, they generally have higher dielectric constants than organic materials.[10,41] Figure 10b shows a plot of the dielectric constant vs the SWNT concentration for the composites. The dielectric constant of the pristine SWNT composite kept increasing with increasing CNT concentration and was 1.7-fold greater for the composite with 0.1 wt % of SWNTs compared with the bare one.

Conclusions

The method reported herein provides a facile way to prepare a polymeric CNT−LC composite that combines the properties of both LCs and SWNTs. We utilized the LC-state polymerization for the composite preparation. The SWNTs were dispersed in a lyotropic LC of a polymerizable surfactant, which allowed them to be incorporated into the hexagonal structure of the LC. The photopolymerization of the LC mixture produced a mechanically stable, polymeric SWNT−LC composite. After polymerization, the structure was changed from columnar hexagonal to lamellar. We believe this method has a great potential for the preparation of composite materials with novel functionality and enhanced electrical, mechanical, and thermal properties, due to the presence of well-dispersed and aligned CNTs.

Acknowledgment. This work was supported by the grant from the Global Research Lab program of Ministry of Education, Science and Technology, Korea.

References and Notes

(1) Sinnott, S. B.; Andrews, R. *Crit. Rev. Solid State Mater. Sci.* **2001**, *26*, 145–249.
(2) Joselevich, E. *ChemPhysChem* **2004**, *5*, 619–624.
(3) Dresselhaus, M. S.; Dresselhaus, G..; Saito, R. *Carbon* **1995**, *33*, 883–891.
(4) Eklund, P. C.; Holden, J. M.; Jishi, R. A. *Carbon* **1995**, *33*, 957–972.
(5) Miyauchi, Y.; Oba, M.; Maruyamag, S. *Phys. Rev. B* **2006**, *74*, 205440.
(6) Pop, E.; Mann, D.; Wang, Q.; Goodson, K.; Dai, H. *Nano Lett.* **2006**, *6*, 96–100.
(7) Peng, H.; Sun, X. *Chem. Phys. Lett.* **2009**, *471*, 103–105.
(8) Gao, L.; Zhou, X.; Ding, Y. *Chem. Phys. Lett.* **2007**, *434*, 297–300.
(9) Du, F.; Fischer, J. E.; Winey, K. I. *J. Polym. Sci., Part B: Polym. Phys. Ed.* **2003**, *41*, 3333–3338.
(10) Clayton, L. M.; Sikder, A. K.; Kumar, A.; Cinke, M.; Meyyappan, M.; Gerasimov, T. G.; Harmon, J. P. *Adv. Funct. Mater.* **2005**, *15*, 101–106.
(11) Thess, A.; Lee, R.; Nikolaev, P.; Dai, H. J.; Petit, P.; Robert, J.; Xu, C. H.; Lee, Y. H.; Kim, S. G.; Rinzler, A. G.; Colbert, D. T.; Scuseria, G. E.; Tomanek, D.; Fischer, J. E.; Smalley, R. E. *Science* **1996**, *273*, 483–487.
(12) Villmow, T.; Pötschke, P.; Pegel, S.; Häussler, L.; Kretzschmar, B. *Polymer* **2008**, *49*, 3500–3509.
(13) Wang, L.; Choi, H.; Myoung, J.; Lee, W. *Carbon* **2009**, *47*, 3427–3433.
(14) Moore, V. C.; Strano, M. S.; Haroz, E. H.; Hauge, R. H.; Smalley, R. E.; Schmidt, J.; Talmon, Y. *Nano Lett.* **2003**, *3*, 1379–1382.
(15) Wang, Q.; Han, Y.; Wang, Y.; Qin, Y.; Guo, Z. *J. Phys. Chem. B* **2008**, *112*, 7227–7233.
(16) Guldi, D. M.; Rahman, G. M. A.; Jux, N.; Balbinot, D.; Hartnagel, U.; Tagmatarchis, N.; Prato, M. *J. Am. Chem. Soc.* **2005**, *127*, 9830–9838.

(17) Badaire, S.; Zakri, C.; Maugey, M.; Derré, A.; Barisci, J. N.; Wallace, G..; Poulin, P. *Adv. Mater.* **2005**, *17*, 1673–1676.
(18) Moulton, S. E.; Maugey, M.; Poulin, P.; Wallace, G. G. *J. Am. Chem. Soc.* **2007**, *129*, 9452–9457.
(19) Hirsch, A. *Angew. Chem., Int. Ed.* **2002**, *41*, 1853–1859.
(20) Balasubramanian, K.; Burghard, M. *Small* **2005**, *1*, 180–192.
(21) Georgakilas, V.; Tagmatarchis, N.; Pantarotto, D.; Bianco, A.; Briand, J.; Prato, M. *Chem. Commun.* **2002**, *24*, 3050–3051.
(22) Ramanathan, T.; Fisher, F. T.; Ruoff, R. S.; Brinson, L. C. *Chem. Mater.* **2005**, *17*, 1290–1295.
(23) Park, C.; Wilkinson, J.; Banda, S.; Ounaies, Z.; Wise, K. E.; Sauti, G.; Lillehei, P. T.; Harrison, J. S. *J. Polym. Sci., Part B: Polym. Phys. Ed.* **2006**, *44*, 1751–1762.
(24) Ge, J. J.; Hou, H.; Li, Q.; Graham, M. J.; Greiner, A.; Reneker, D. H.; Harris, F. W.; Cheng, S. Z. D. *J. Am. Chem. Soc.* **2004**, *126*, 15754–15761.
(25) Gao, J.; Yu, A.; Itkis, M. E.; Bekyarova, E.; Zhao, B.; Niyogi, S.; Haddon, R. C. *J. Am. Chem. Soc.* **2004**, *126*, 16698–16699.
(26) Xu, J.; Florkowski, W.; Gerhardt, R.; Moon, K. S.; Wong, C. P. *J. Phys. Chem. B* **2006**, *110*, 12289–12292.
(27) Weiss, V.; Thiruvengadathan, R.; Regev, O. *Langmuir* **2006**, *22*, 854–856.
(28) Scalia, G.; Bühler, C.; Hägele, C.; Roth, S.; Giesselmann, F.; Lagerwall, J. *Soft Matter* **2008**, *4*, 570–576.
(29) Lagerwall, J.; Scalia, G.; Haluska, M.; Dettlaff-Weglikowska, U.; Roth, S.; Giesselmann, F. *Adv. Mater.* **2007**, *19*, 359–364.
(30) Jiang, W.; Yu, B.; Liu, W.; Hao, J. *Langmuir* **2007**, *23*, 8549–8553.
(31) Kumar, S.; Bisoyi, H. K. *Angew. Chem., Int. Ed.* **2007**, *46*, 1501–1503.
(32) Bisoyi, H. K.; Kumar, S. *J. Mater. Chem.* **2008**, *18*, 3032–3039.
(33) Dierking, I.; Scalia, G.; Morales, P.; LeClere, D. *Adv. Mater.* **2004**, *16*, 865–869.
(34) Kimura, M.; Miki, N.; Adachi, N.; Tatewaki, Y.; Ohta, K.; Shirai, H. *J. Mater. Chem.* **2009**, *19*, 1086–1092.
(35) Kumar, S.; Dang, T. D.; Arnold, F. E.; Bhattacharyya, A. R.; Min, B. G.; Zhang, X.; Vaia, R. A.; Park, C.; Adams, W. W.; Hauge, R. H.; Smalley, R. E.; Ramesh, S.; Willis, P. A. *Macromolecules* **2002**, *35*, 9039–9043.
(36) Jang, J.; Bae, J.; Yoon, S. *J. Mater. Chem.* **2003**, *13*, 676–681.
(37) Meuer, S.; Braun, L.; Zentel, R. *Chem. Commun.* **2008**, *27*, 3166–3168.
(38) Nagai, K.; Ohishi, Y.; Inaba, H.; Kudo, S. *J. Polym. Sci., Part A: Polym. Chem. Ed.* **1985**, *23*, 1221–1230.
(39) McGrath, K. M.; Drummond, C. *J. Colloid Polym. Sci.* **1996**, *274*, 612–621.
(40) Sievens-Figueroa, L.; Guymon, C. A. *Polymer* **2008**, *49*, 2260–2267.
(41) Li, Q.; Xue, Q.; Zheng, Q.; Hao, L.; Gao, X. *Mater. Lett.* **2008**, *62*, 4229–4231.